

---

EFDA–JET–CP(02)07/07

T.C. Hender, O. Sauter, B. Alper, C. Angioni, M.de Baar, M.De Benedetti, P. Belo, M. Bigi, D.N. Borba, T. Bolzonella, R. Budny, R.J. Buttery, A. Gondhalekar, N.N. Gorelenkov, A. Gude, S. Guenter, T. Hellsten, D.F. Howell, R. Koslowki, R.J. La Haye, A.W. Hyatt, P. Lamalle, E. Lazzaro, M.J. Mantsinen, M. Maraschek, M.L. Mayoral, K.G. McClements, F. Milani<sup>1</sup>, F. Nabais, M.F.F. Nave, F. Nguyen, S. Nowak, A.-L. Pecquet, C.C. Petty, S.D. Pinches, A. Pochelon, S. Podda, C. Perez von Thun, J. Rapp, F. Salzedas, F. Sartori, S.E. Sharapov, M. Stamp, D. Testa, E. Westerhof, P.de Vries and P. Zanca

# Sawtooth, Neo-Classical Tearing Mode and Error Field Studies in JET



# Sawtooth, Neo-Classical Tearing Mode and Error Field Studies in JET

T.C. Hender<sup>1</sup>, O. Sauter<sup>2</sup>, B. Alper<sup>1</sup>, C. Angioni<sup>2</sup>, M.de Baar<sup>3</sup>, M.De Benedetti<sup>4</sup>, P. Belo<sup>5</sup>,  
M. Bigi<sup>1</sup>, D.N. Borba<sup>5,6</sup>, T. Bolzonella<sup>7</sup>, R. Budny<sup>8</sup>, R.J. Buttery<sup>1</sup>, A. Gondhalekar<sup>1</sup>,  
N.N. Gorelenkov<sup>8</sup>, A. Gude<sup>9</sup>, S. Guenter<sup>9</sup>, T. Hellsten<sup>10,6</sup>, D.F. Howell<sup>1</sup>, R. Koslowki<sup>11</sup>,  
R.J. La Haye<sup>12</sup>, A.W. Hyatt<sup>12</sup>, P. Lamalle<sup>13,6</sup>, E. Lazzaro<sup>14</sup>, M.J. Mantsinen<sup>15</sup>,  
M. Maraschek<sup>9</sup>, M.L. Mayoral<sup>1</sup>, K.G. McClements<sup>1</sup>, F. Milani<sup>1</sup>, F. Nabais<sup>5</sup>, M.F.F. Nave<sup>5</sup>,  
F. Nguyen<sup>16</sup>, S. Nowak<sup>14</sup>, A.-L. Pecquet<sup>16</sup>, C. Perez von Thun<sup>11</sup>, C.C. Petty<sup>12</sup>,  
S.D. Pinches<sup>9</sup>, A. Pochelon<sup>2</sup>, S. Podda<sup>4</sup>, J. Rapp<sup>11,6</sup>, F. Salzedas<sup>5</sup>, F. Sartori<sup>1</sup>,  
S.E. Sharapov<sup>1</sup>, M. Stamp<sup>1</sup>, D. Testa<sup>17,2</sup>, E. Westerhof<sup>3</sup>, P.de Vries<sup>3</sup>, P. Zanca<sup>7</sup>  
and contributors to the EFDA-JET workprogramme\*

<sup>1</sup>Euratom/UKAEA Fusion Association, Culham Science Centre, Abingdon, OX14 3DB, UK;

<sup>2</sup>CRPP, Assoc. Euratom-Confédération Suisse, École Polytechnique Fédérale de Lausanne (EPFL), Switzerland

<sup>3</sup>Associatie Euratom -FOM, Nieuwegein, Netherlands

<sup>4</sup>CRE ENEA, Assoc. EURATOM-ENEA, Frascati, Italy

<sup>5</sup>Assoc. Euratom/IST, Centro de Fusão Nuclear, Lisboa, Portugal

<sup>6</sup>EFDA-JET CSU, Culham Science Centre, Abingdon, Oxfordshire, UK;

<sup>7</sup>Consorzio RFX Assoc. Euratom-ENEA-CNR, Padova, Italy

<sup>8</sup>PPPL, Princeton, NJ, USA;

<sup>9</sup>IPP-Euratom Assoziation, Garching, Germany

<sup>10</sup>KTH Assoc. Euratom/NFR, Stockholm, Sweden

<sup>11</sup>Forschungszentrum Jülich GmbH, Euratom Association, Jülich, Germany;

<sup>12</sup>General Atomics, San Diego, USA

<sup>13</sup>ERM/KMS, Euratom-Belgian State Assoc. Brussels, Belgium

<sup>14</sup>IFP CNR Assoc. Euratom-ENEA-CNR, Milan, Italy

<sup>15</sup>Helsinki University of Technology, Association Euratom-Tekes, Finland

<sup>16</sup>Association Euratom-CEA sur la Fusion Contrôlée, Cadarache, France

<sup>17</sup>PSFC, MIT, Cambridge, USA

\* See annex of J. Pamela et al, "Overview of Recent JET Results and Future Perspectives",  
Fusion Energy 2000 (Proc. 18<sup>th</sup> Int. Conf. Sorrento, 2000), IAEA, Vienna (2001).

“This document is intended for publication in the open literature. It is made available on the understanding that it may not be further circulated and extracts or references may not be published prior to publication of the original when applicable, or without the consent of the Publications Officer, EFDA, Culham Science Centre, Abingdon, Oxon, OX14 3DB, UK.”

“Enquiries about Copyright and reproduction should be addressed to the Publications Officer, EFDA, Culham Science Centre, Abingdon, Oxon, OX14 3DB, UK.”

## ABSTRACT.

A range of ITER relevant plasma stability issues has been studied in the JET tokamak; these include the effects of fast particles on sawteeth, control of NTMs via sawtooth seeds, scaling of  $m=2, n=1$  NTM thresholds and the effect of error fields on plasma rotation and vice-versa. The sawtooth studies have examined both the effects of ICRF and NBI fast particles, and models used for ITER predictions have been validated. Large sawteeth, due to fast particle stabilisation, have been shown to trigger  $m=3, n=2$  NTMs at low beta. Conversely the use of ICCD to produce small short period sawteeth has been shown to raise the NTM b-limit, suggesting the value of local current drive near  $q=1$ . The marginal-b ( $b_{N,marg}$ ) below which the  $m=3, n=2$  NTM is unconditionally stable has been examined; it is found that  $b_{N,marg}$  scales almost linearly with  $r^*$  and typical H-mode (with  $q_{95} \approx 3$ ) discharges are meta-stable to NTMs (ie a sufficiently large seed can always destabilise an NTM). The  $m=2, n=1$  NTM has been studied in a joint scaling experiment with the DIII-D tokamak. These experiments, using closely matched non-dimensional parameters (plasma shape,  $R/a$ ,  $q$ , gyro-radius and collisionality) on DIII-D and JET, show similar NTM b-limits and consistent scalings. The issue of error field thresholds and their variation with plasma rotation has also been studied, helping to clarify scalings to ITER.

## 1. INTRODUCTION

Studies on JET with 3<sup>rd</sup> harmonic  $^4\text{He}$  ion cyclotron resonance heating (ICRH) [1], simulating  $\alpha$ -particles, have shown that the resulting fast particle stabilisation of the sawteeth can lead to long sawtooth periods and large crashes which trigger neo-classical tearing modes (NTMs) at low normalised  $\beta_N$  [2]. More generally a clear operational relation is found to exist between sawtooth period and the 3/2 ( $m=3, n=2$ ) NTM  $\beta$ -limit (Fig 1).

Since NTMs can result in a 10-20% confinement degradation, it is important to explore both the fast particle stabilisation of sawteeth and means to avoid long period sawteeth, to optimise NTM stability. Such issues have been examined in the JET tokamak over the past 2 years; in addition other important physics issues (e.g. seeding and scalings) have been studied for NTMs, to improve extrapolations to ITER, as have the thresholds for error fields to induce locked modes.

## 2. FAST PARTICLE EFFECTS ON SAWTEETH

The studies of the effects of fast particles on sawteeth have been conducted in JET using both deuterium neutral beam injection (NBI) and ICRH. The NBI studies show a hysteresis of the sawtooth period with respect to power (Fig 2), which is consistent with the slowing down time of the fast NBI ions. In order to investigate a possible theoretical basis for the observed sawtooth period behaviour with NBI, a model [3] which was developed to predict behaviour in ITER, has been applied [4]. An analytic beam ion contribution to the internal kink potential energy, validated using the hybrid kinetic/MHD code NOVA-K [5], has been implemented in the transport code PRETOR [6]. The beam ion term is found to be sufficiently stabilising to produce simulated sawtooth periods

in agreement with the experimental results (without this term sawtooth periods are much shorter than the measured periods). The model indicates that sawteeth are triggered in these JET discharges by excitation of the internal kink in the semi-collisional ion-kinetic regime; thought to be the most relevant regime for ITER. These calculations thus serve as a validation of the methodology used to predict ITER sawtooth periods.

For ICRH, previous studies on JET [7], and the recent  $^4\text{He}$  experiments mentioned in the Introduction, have shown the stabilising effect from the ICRH fast ion population. Recent studies have also focussed on the effects of  $\omega \approx 2\omega_{\text{CH}}$  H-minority ion cyclotron heating and current drive (ICCD) on sawteeth [8], with both low and high field side (HFS) resonances examined [9]. The shape of the calculated current perturbation and the radial localisation of the heating power density for the LFS resonance are consistent with the experimentally observed evolution of the sawtooth period when the resonance layer moves near the  $q=1$  surface; in particular it is found that sawteeth are destabilised, with a minimum period, when the ICCD is just inside the sawtooth inversion radius. The diamagnetic current driven near  $q=1$  is calculated to be similar with  $\pm 90^\circ$  phasing [10] and experimentally little difference is observed. Similar results are obtained for HFS resonances with the sawtooth period being minimised when the resonance is just inside the sawtooth inversion radius with  $-90^\circ$  phasing (Fig 3).

### 3. NTM CONTROL

Since sawteeth are the primary seed for  $3/2$  NTMs their control with ICCD has been exploited to delay, or prevent, NTM onset. By active sawtooth destabilisation, short period and low amplitude sawteeth are generated, such that the sawtooth produced NTM seed island is reduced and the threshold normalised- $\beta$  for triggering of  $3/2$  NTMs,  $\beta_{\text{N onset}}$ , is increased (Fig 4).

This is an important result for ITER, suggesting the benefit of sawtooth destabilisation, via local current drive, to counter  $\alpha$ -particle stabilisation. This technique might use ECCD or ICCD near  $q=1$ , and should retain the beneficial properties of sawteeth in limiting core He-ash accumulation. The converse of these results is that, in general, large sawteeth can induce NTMs whenever there is an H-mode in JET; this is confirmed by power ramp-down studies which show the  $3/2$  NTM only stabilises at, or close to, the H-L transition (see next section). It should be noted that, although the link between sawteeth, their control and NTM seeding is clearly established, the exact seeding mechanism is not clear in all cases; when the  $3/2$  NTM is seeded it is generally not phased locked to the  $2/2$  nonlinear side-band of the  $1/1$  mode, nor is it always clearly driven by triplet coupling with the  $4/3$  mode which precedes the  $3/2$ .

### 4. NTM PHYSICS STUDIES

The onset of an NTM instability is governed both by its intrinsic stability and by the size of the seed islands available to initiate its growth. However, once initiated, studies ramping down the additional heating power generally show a large hysteresis in  $b$  before the NTM is stabilised. The marginal

normalised  $\beta$  ( $\beta_{N,\text{marg}}$ ) below which the NTM is unconditionally stable is governed solely by the intrinsic NTM stability and not by seed island effects; hence studies of NTM marginal stability can directly address the form of the equation governing NTM stability and in particular the nature of the small island width stabilising terms. The modified Rutherford equation determines the NTM island width ( $w$ ) evolution [12]:

$$\frac{dw}{dt} \propto \Delta' + \beta_p \left( \frac{a_{bs}}{w^2 + w_d^2} + \frac{a_{GGJ}}{\sqrt{w^2 + 0.2w_d^2}} + \frac{a_{pol} w}{w^4 + w_d^4} \right) \quad (1)$$

where  $\Delta'$  is the tearing stability parameter, the  $a_{bs}$  term is the bootstrap drive term which is reduced at small  $w$  due to the finite perpendicular transport [13], the  $a_{GGJ}$  term is the curvature effect and the  $a_{pol}$  term is due to the polarisation current effect [14]. Experiments have been performed, slowly ramping down the ICRH/NBI power once a 3/2 NTM is formed; these experiments frequently exploit real time detection of the NTM, and control of the heating power. The 3/2 island width evolution for a typical 2.7MA/2.7T discharge, in which the power is ramped down, is shown in Fig 5. Also shown is predicted evolution from a slightly more general form of Eq (1) [15] including  $\chi_{\perp}$  stabilising terms only, polarisation stabilisation terms only and both terms. The island width evolution is generally well modelled by both stabilising effects but close examination shows the  $\chi_{\perp}$ -model is appropriate to explain the island decay in the 4-6cm range while the polarisation model terms are needed to explain the rapid decay for  $\beta < \beta_{\text{marg}}$ . For typical H-modes in JET, with  $q_{95} \approx 3.3$ , it is found that the 3/2 NTM is stabilised near the H-L transition, though at higher  $q_{95}$  NTM stabilisation occurs while the discharge is still in H-mode. At lower  $q_{95}$  ( $\approx 2.5$ ) a similar  $\beta_{N,\text{marg}}$  is found, suggesting that the lower onset  $\beta_N$  at  $q_{95} < 3$ , that has been previously reported [16], is due to a stronger coupling with the sawtooth seed. Initial studies indicate that  $\beta_{N,\text{marg}} \propto \rho^{*1.1}$  and is independent of collisionality. Such a scaling indicates H-modes in ITER will always be metastable to 3/2 NTMs thus highlighting the value of current drive control of the seed islands in ITER.

The onset scalings for the  $m=2, n=1$  NTM have also been studied in a joint experiment between JET and DIII-D. The 2/1 NTM has potentially serious consequences as it always leads to severe energy confinement degradation and can lead to disruptions. Very similar instability behaviour is observed on both JET and DIII-D as shown in Fig 6.

These 2/1 modes are identified as NTMs from the observation of  $n=1$  islands at  $q=2$  and from the scaling of the mode island width with  $\beta$ , including a substantial hysteresis between the onset and marginal  $\beta$ 's. Similarity experiments using closely matched non-dimensional parameters (plasma shape, aspect ratio,  $q$ ,  $\rho^*$  and collisionality) on the 2 machines show similar global  $\beta$ -limits for the NTM (Fig 7).

Consistent scalings for the onset of the 2/1 NTM (including standard plasma shape DIII-D data) are found between JET and DIII-D. For example it is found that thermal- $\beta_N$  at 2/1 onset scales as  $\beta_N \propto (\rho^*)^{1.02} (v^*)^{0.19}$ , which is very similar to the scaling for the 3/2 NTM and indicates the importance of considering control schemes for the 2/1 NTM in next generation tokamaks.

## 5. LOCKED MODES

The (2,1) NTMs frequently result in a locked or nearly locked mode. The converse problem of how the approach to NTM stability affects the threshold for error fields to form locked modes is also being studied; initial results show a marked decrease in threshold as the (2,1) NTM  $\beta_N$  limit is approached. More generally the issue of error field thresholds and their variation with plasma rotation has been studied. This is an important issue for ITER, where the increased sensitivity to error fields at high toroidal field ( $B_{\text{thresh}}/B_t \propto B_t^{-1.2}$  from JET scaling studies), has shown it is prudent to include an error field correction system. It is found that an improved description of the data is obtained by including a theoretically predicted form of the plasma rotation into the scaling for the threshold error field to form an  $m=2, n=1$  locked mode; in particular it is found that the locked mode threshold is well described by the scaling relation  $B_{\text{thresh}}/B_t \propto n^{0.58} B_t^{-1.27} \omega_0^{1/2}$  (where  $\omega_0$  is the pre-error field fluid rotation frequency at  $q=2$ ). Further, a good match to theory has been achieved, with locked mode formation being precipitated after the EM torque has slowed the plasma to  $1/2$  its original frequency. The results have also shed light on the important physics of plasma rotation braking from applied helical ‘error fields’. A viscous drag model with the torque applied solely at the island ( $q=2$ ) surface would predict a uniform reduction of the rotation within  $q=2$ , but the observations seem to contradict this and indicate an approximately self-similar reduction of plasma rotation within  $q=2$  (Fig 8).

A new model associated with a toroidal viscous drag originating from non-axisymmetric fields, in particular due to the non-resonant  $m=0, n=1$  mode, seems to qualitatively match these observations [17], however a more complete treatment including mode coupling due to toroidal and shaping effects [18] is needed to fully understand the fluid rotation behaviour.

## 6. SUMMARY AND FUTURE PROSPECTS

$3/2$  NTMs are likely to be metastable in ITER H-mode operation and could be triggered by the crash of long period sawteeth (e.g. due to a-particle stabilisation), emphasising the value of developing NTM control schemes. Such schemes should include current drive control of the sawteeth using ECCD or ICCD. Physics studies of the  $3/2$  NTM in JET have clarified the likely role played by both perpendicular transport and polarisation currents in setting a finite island width threshold for NTM growth. The  $m=2, n=1$  NTM has been studied in a joint scaling experiment with the DIII-D tokamak. These experiments using closely matched non-dimensional parameters on DIII-D and JET show similar NTM  $\beta$ -limits. Also the data from the 2 machines is well represented by scalings indicating an approximately linear scaling of the onset- $\beta$  with  $\rho^*$ ; showing the value of  $2/1$  NTM control for future devices. However, further studies on seeding and  $2/1$  NTM physics, similar to the  $3/2$  studies, are needed to assess the implications for ITER.

The increased sensitivity to the formation of error field locked modes as  $B_t$  increases, has led to the inclusion of error field correction coils in the ITER design. Further error field studies on JET have refined the threshold scaling expressions and shed further light on how error fields interact to



slow the plasma rotation. A new mechanism based on the drag from non-resonant harmonics has been proposed, which may supplement toroidal coupling effects in determining the bulk slowing of plasma rotation. In the near future it is planned to study direct control of the NTMs at  $q=3/2$  and  $2/1$  by LHCD and ICCD; studies which should benefit from the planned increase of NBI power. Error field locked mode studies exploiting the newly installed Error Field Correction Coils will continue with particular emphasis on the effects of error fields at high- $b$ . Thus JET studies will continue to make important contributions to the understanding of MHD instabilities, and their control, for ITER.

## ACKNOWLEDGEMENT

This work was conducted under the European Fusion Development Agreement and partly funded by EURATOM and UK Department of Trade and Industry.

## REFERENCES

- [1]. M J Mantsinen et al, Phys Rev Lett **88** (2002) 105002-1
- [2]. J Pamela et al, Nucl Fus **42** (2002) 1014
- [3]. F Porcelli et al, Plasma Phys and Contr Fus **38** (1996) 2163
- [4]. C Angioni et al, Plasma Phys and Contr Fus **44** (2002) 1521
- [5]. N N Gorelenkov et al, Phys Plasmas **6** (1999) 2802
- [6]. D Boucher et al, Proc IAEA Tech Com. Meeting on Advances in Simulation and Modelling of Thermo-nuclear Plasmas, 1992 Montreal (1993) p142.
- [7]. D J Campbell et al, Phys Rev Lett **60** (1988) 2148
- [8]. Angioni C. et al., 29th EPS Conf on Plasma Phys. and Contr. Fusion, Montreux, 17-21 June 2002, ECA Vol. 26B, P-1.118 (2002)
- [9]. M-L Mayoral et al, 29th EPS Conf on Plasma Phys. and Contr. Fusion, Montreux, 17-21 June 2002, ECA Vol. 26B, P-1.026 (2002)
- [10]. M Mantsinen et al, Plasma Phys and Control Fus **8** (2002) 1521
- [11]. O Sauter et al, Phys. Rev. Lett., **88** (2002) 105001.
- [12]. O Sauter et al, Phys Plasmas **4** (1997) 1654
- [13]. R Fitzpatrick et al, Phys Plasmas **2** (1995) 825 and N N Gorelenkov et al, Phys Plasmas **3** (1996) 3379.
- [14]. H R Wilson et al, Phys Plasmas **3** (1996) 248
- [15]. O Sauter et al, Plasma Phys and Contr. Fus **44** (2002) 1999
- [16]. T C Hender et al, IAEA 2000 proceedings IAEA-CN-77 XXP3/02 IAEA Vienna (2001) IAEA-CSP-8/C (CD-ROM)
- [17]. E Lazzaro et al, Phys of Plasmas **9** (2002) 3906.
- [18]. E Lazzaro et al, 29th EPS Conf on Plasma Phys. and Contr. Fusion, Montreux, 17-21 June 2002, ECA Vol. 26B, P-5.079 (2002)

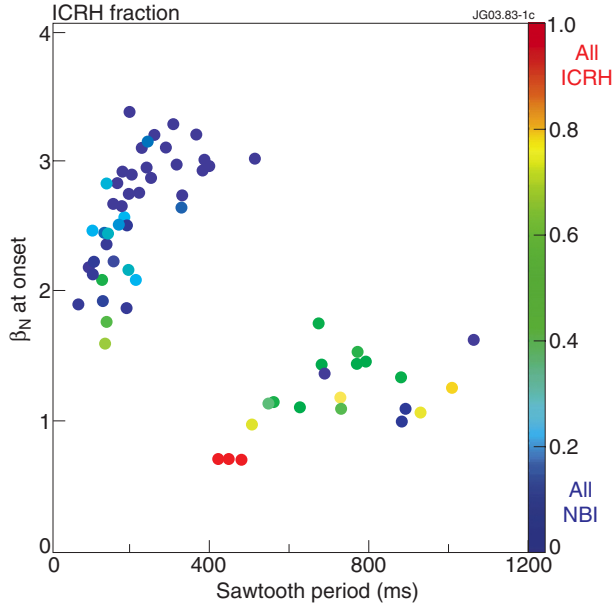


Figure 1: Relation of the  $\beta$ -limit for the 3/2 NTM onset with the period of the immediately preceding sawtooth. Here data with elongations in the range  $1.6 < \kappa < 1.8$  and  $3 < q_95 < 3.5$  are considered. In general the long sawtooth periods correspond to a high ICRH fraction of additional heating power, though there are examples of long sawteeth occurring as the NBI power is switched-on.

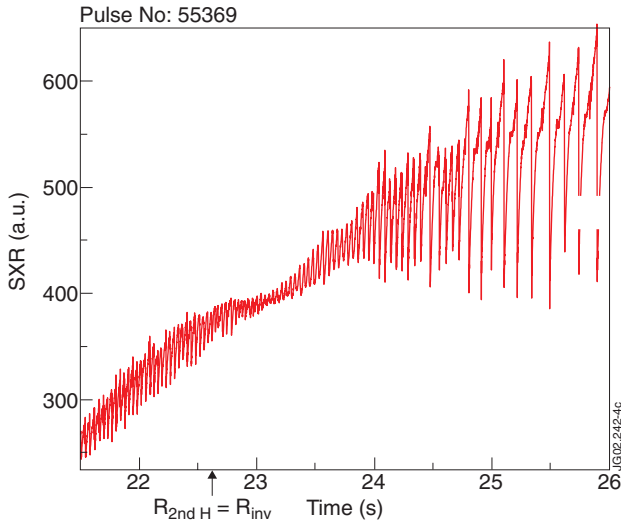


Figure 3: Central SXR chord showing small indistinct sawteeth ( $t \sim 23.5$ s) obtained when the 2<sup>nd</sup> harmonic  $H$ -minority resonance is just inside the sawtooth inversion radius; here the antenna phasing is  $-90^\circ$ . For resonance locations closer to the magnetic axis the fast ion pressure is stabilising, leading to large sawteeth, though still considerably shorter in period than those obtained with  $+90^\circ$  phasing in otherwise comparable conditions.

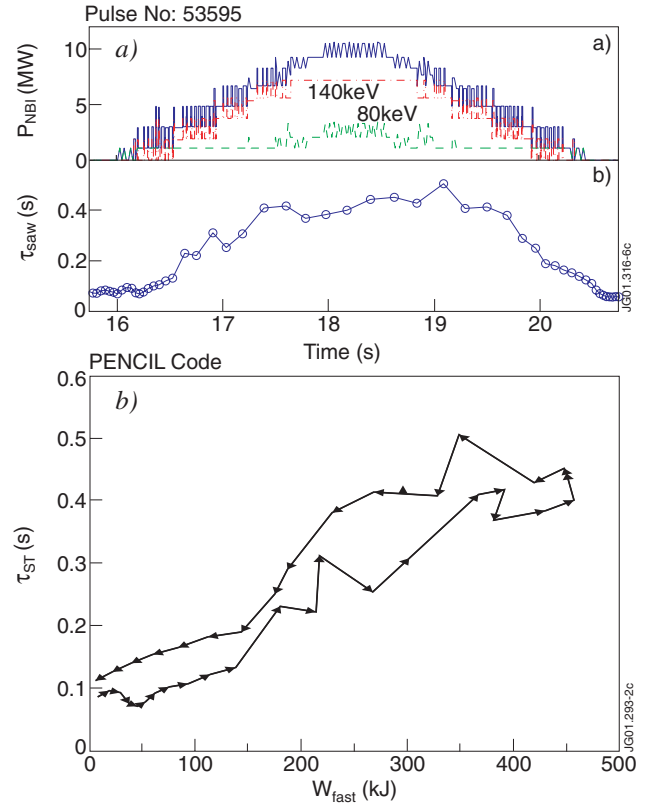


Figure 2(a): Asymmetric variation of sawtooth period (lower trace) resulting from a symmetric ramp-up and down of the NBI power (upper trace). (b) The hysteresis in sawtooth period, with NBI power, is reduced if the sawtooth period as a function of fast particle energy is considered.

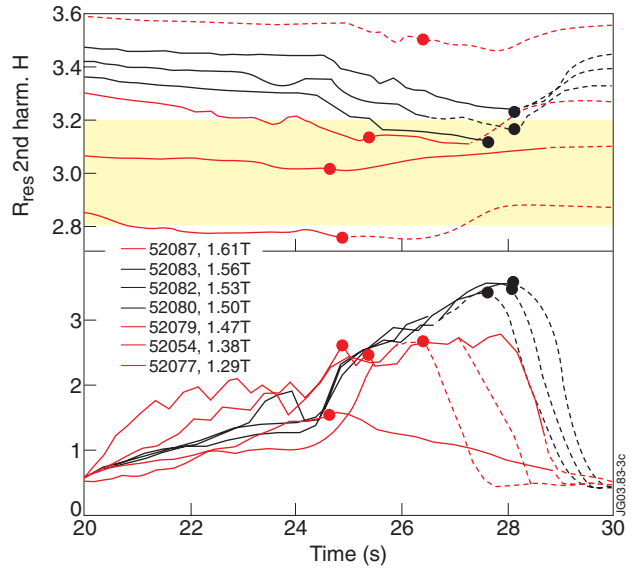


Figure 4: How the NTM onset (marked by the solid dots) varies with LFS ICRF resonance location (upper plot where shaded region marks the radii within the sawtooth inversion radius). It can be seen that  $\beta$  is maximised for discharges with the ICCD located just at the inversion radius. Generally ICRF coupling degrades (dashed lines indicate  $P_{ICRF} < 1$  MW) and diamagnetic effects cause the ICRF resonance to shift inwards, as  $\beta$  rises. Reprinted from Ref [11].

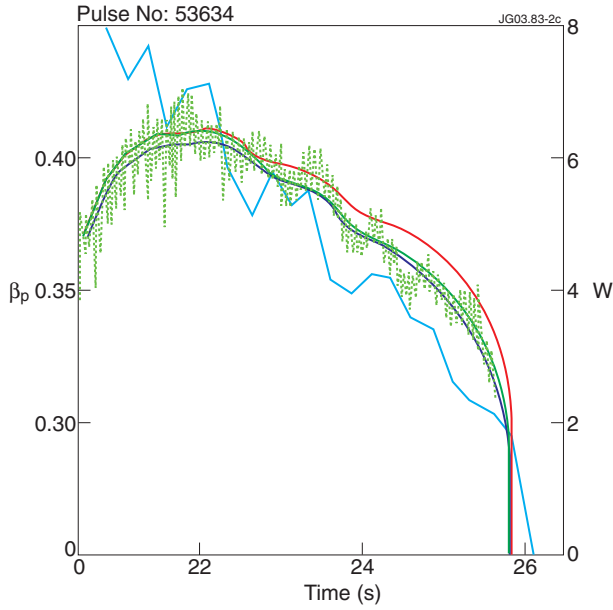


Figure 5: The variation of poloidal- $\beta$  (cyan curve), and the simulated island width (cm) including just the polarisation term (magenta), just the  $\chi_{\perp}$  term (blue) and both stabilising terms (green).

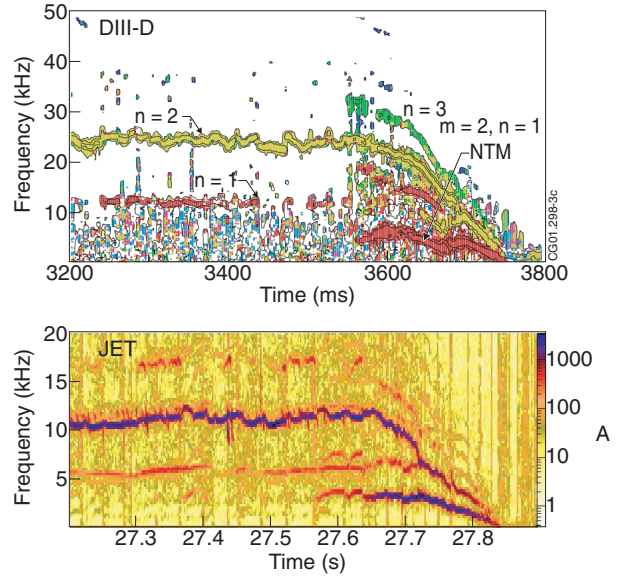


Figure 6: Spectrograms for poloidal Mirnov probes on DIII-D (upper plot) and JET (lower plot). As the power is ramped, first a 3/2 NTM is destabilised (marked  $n=2$ ) and then a 2/1 NTM is destabilised, which slows rapidly to form a large locked (or very slowly rotating) mode. The strong equivalence of the instability behaviour in JET and DIII-D is evident.

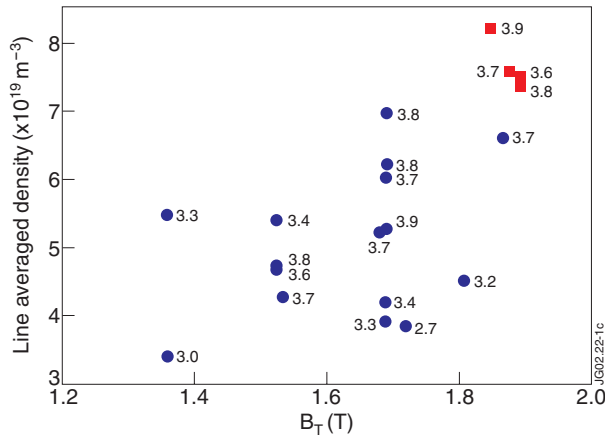


Figure 7: JET shape DIII-D plasma data for the onset of the (2,1) NTM (circles) and some JET cases scaled at constant  $\rho^*$ ,  $\nu^*$  and  $\beta_N$  to DIII-D dimensions (squares). The  $b_N$  is indicated for each case

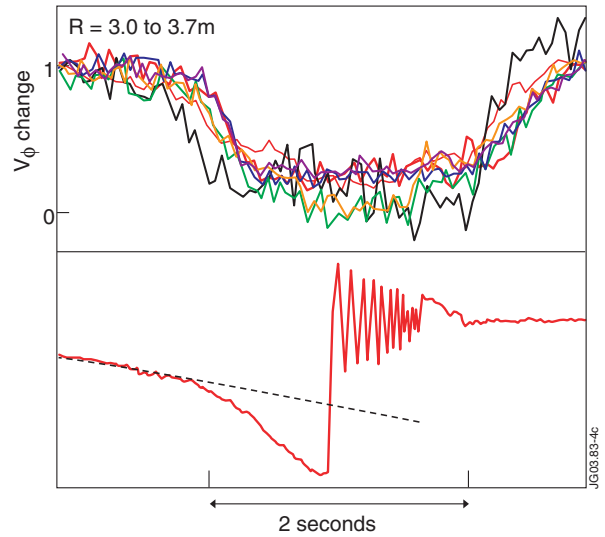


Figure 8: Upper plot:- toroidal velocity (normalised to its value just before the error field is applied) for radii within  $q=2$ . Lower plot:- Measured radial magnetic field. The error field locked mode is induced when this signal departs from linear ramp (indicated by the broken line) expected from a direct response to linearly ramped error field. As the error field is turned off a slowly rotating island occurs, which slowly decays and increases in frequency. The plasma toroidal velocity then approximately returns to its initial value.